Materials Today: Proceedings 42 (2021) 63–68

Contents lists available at ScienceDirect

Materials Today: Proceedings

journal homepage: www.elsevier.com/locate/matpr

# Extracted γ-$Al_2O_3$ from aluminum dross as a catalyst support for glycerol dry reforming reaction

Nurul Asmawati Roslan [a], Sumaiya Zainal Abidin [a,b,*], Nur Shafiqah Nasir [a], Chin Sim Yee [a,b], Y.H. Taufiq-Yap [c,d]

[a] Department of Chemical Engineering, College of Engineering, Universiti Malaysia Pahang, Lebuhraya Tun Razak, 26300 Gambang, Kuantan, Pahang, Malaysia
[b] Centre of Excellence for Advanced Research in Fluid Flow (CARIFF), Universiti Malaysia Pahang, 26300 Gambang, Pahang, Malaysia
[c] Catalysis Science and Technology Research Centre (PutraCAT), Faculty of Science, Universiti Putra Malaysia, 43400, UPM, Serdang, Selangor, Malaysia
[d] Chancellery Office, Universiti Malaysia Sabah, 88400 Kota Kinabalu, Sabah, Malaysia

ARTICLE INFO

*Article history:*
Received 3 July 2020
Received in revised form 2 September 2020
Accepted 16 September 2020
Available online 8 January 2021

*Keywords:*
Aluminum Dross
γ-$Al_2O_3$
Catalyst support
Glycerol Dry Reforming
Syngas

ABSTRACT

The utilization of extracted γ-$Al_2O_3$ (EGA) from aluminum dross as catalyst support in glycerol dry reforming reaction (GDR) has been investigated in this current study. In this study, three main stages were evaluated which are; (i) extraction of γ-$Al_2O_3$; (ii) preparation and characterizations of Ni-based catalyst supported on EGA and (iii) utilization of EGA as catalyst support in the GDR reaction. In the first stage, γ-$Al_2O_3$ with the specific surface area of 156.5 $m^2 g^{-1}$ was successfully extracted before used as catalyst support. Then, 10%Ni/EGA catalyst with 108.3 $m^2 g^{-1}$ surface area was prepared by wet impregnation method. The glycerol conversion and hydrogen yield achieved in the third stage were 22% and 15% respectively. The results can be attributed to the high specific surface area of EGA, which enhanced the dispersion of Ni particles on the catalyst matrix.
© 2019 Elsevier Ltd. All rights reserved.
Selection and Peer-review under responsibility of the scientific committee of the International Conference of Chemical Engineering & Industrial Biotechnology.

## 1. Introduction

Glycerol dry reforming (GDR) has been one of the alternative routes to produce CO and $H_2$ (i.e. known as syngas) with $H_2$ as the main constituent. The utilization of greenhouse gas (i.e. $CO_2$) and glycerol as a by-product from biodiesel industry could potentially reduce the production costs of biodiesel [1], the production of waste [2] and beneficial to the environment. Besides, GDR is preferable compared to steam reforming due to the lower ratio of $H_2$/CO, which is more suitable for the Fischer-Tropsch (FT) process [3]. Ni-based catalyst is widely used in the reforming reaction due to the facts of its lower price, readily available, high selectivity toward the production of $H_2$ and ability to break the C–C bonds [4]. However, the major drawback having by Ni-based catalyst is due to its severe carbon deposition and thus, leading to the deactivation of the catalyst [5,6]. Selection of good catalyst support is one of the potential solutions to overcome the problems as an excellent catalyst support improve the catalyst stability during the reaction. Cao, $SiO_2$, $ZrO_2$, $La_2O_3$ and $Al_2O_3$ were widely used as catalyst support in the reforming process. Among these oxides, $Al_2O_3$ gains considerable interest due to its good metal-support interaction, high mechanical and chemical resistance under severe reaction conditions and high specific surface area [7].

The researchers have gained attention towards the production of $Al_2O_3$ from aluminum dross to reduce the waste volume and the environmental problem. Currently, the global aluminum industry produced more than 1,000,000 tons of hazardous waste, and this includes aluminum dross and its salt cakes [8]. This phenomenon imposed high disposal costs and severe environmental problems [9]. They are two types of aluminum dross which are primary and secondary dross. Primary dross which is presences in clump form contains more than 50% aluminum metal and small compositions of salt and oxidic constituents [10]. Since the amount of aluminum metal is still high, primary dross will be returned to the smelter and recycle. However, secondary dross which contains approximately 15–30% of aluminum metal, was disposed of in landfill sites. This activity caused severe water pollution due to the leaching of toxic metal ions into the groundwater [11]. Besides, the valuable metal presences in the aluminum dross will not fully utilize. Thus, an appropriate recycle technique is needed to reduce environmental pollution, disposal cost, and simultaneously reduc-

* Corresponding author.
*E-mail address:* sumaiya@ump.edu.my (S.Z. Abidin).

https://doi.org/10.1016/j.matpr.2020.09.390
2214-7853/© 2019 Elsevier Ltd. All rights reserved.
Selection and Peer-review under responsibility of the scientific committee of the International Conference of Chemical Engineering & Industrial Biotechnology.

ing the massive waste generation. Also, such promising approaches can result in the economic benefits and conservation of natural sources. Recently, the recovery of high value-added products from aluminum dross such as γ-$Al_2O_3$ has been explored by the researchers worldwide. Usually, the acid leaching technique by $H_2SO_4$ was employed to extract the γ-$Al_2O_3$ from aluminum dross. During the acid leaching process of $H_2SO_4$, the following reactions were occurred [12]:

Acid leaching process:

$$2Al_2O_3(s) + 6H_2SO_4(l) = Al_2(SO_4)_3(l) + 3SO_2(g) + 6H_2O(l) \quad [1]$$

All the inflammable and toxic gaseous were released during the reaction:

$$2Al_2(s) + 3H_2SO_4(l) = Al_2(SO_4)_3(l) + 3H_2(g) \quad [2]$$

$$2AlN(s) + 6H_2O(l) = 2Al(OH)_3(l) + 32NH_3(l) + 2NH_3(g) \quad [3]$$

Reaction between ammonia solution and leached liquor:

$$Al_2(SO_4)_3(l) + 6NH_4OH(l) = 2Al(OH)_3(s) + 3(NH_4)_2SO_4(l) \quad [4]$$

Calcination process:

$$2Al(OH)_3(s) = Al_2O_3(s) + 3H_2O(l) \quad [5]$$

γ-$Al_2O_3$ was widely applied in various industry and commonly used as catalyst support in the reforming process due to its higher surface area and good metal-support interaction [13]. However, none of the literature reported the utilization of γ-$Al_2O_3$ extracted from aluminum dross as catalyst support in the GDR.

Therefore, the GDR reaction using extracted γ-$Al_2O_3$ (EGA) as catalyst support will be investigated in this study. There are two main stages in this study which are (i) the extraction of γ-$Al_2O_3$ from aluminum dross and (ii) the evaluation of the γ-$Al_2O_3$ as a catalyst support in the GDR. In the first stage, the EGA was extracted and characterized. Then, it will be used as catalyst support to prepare the Ni-based catalyst. The Ni-based catalyst supported on EGA produced at this stage was then used in the GDR reaction in the second stage.

## 2. Methodology

Three main stages were developed to investigate the performance of extracted γ-$Al_2O_3$ (EGA) as catalyst support in glycerol dry reforming (GDR) reaction which are; (i) extraction of γ-$Al_2O_3$ from aluminum dross; (ii) catalyst preparation (iii) GDR reaction.

### 2.1. Extraction of γ-$Al_2O_3$ from aluminum dross

In this study, EGA as catalyst support was prepared by acid leaching process. Aluminum dross used in this study was collected from aluminum processing industries in Malaysia. First, the raw dross was mixed with distilled water at a rotational speed of 200 rpm for 30 min. The washed dross was then dried for 12 h in an oven at 60 °C. The washed aluminum dross was then leached with 2 M sulphuric acid in a ratio of dross to the acid of 1:4. The beaker was covered with aluminum foil to prevent spilling of chemicals during the reaction. The leaching process takes place for 1 h at a temperature of 70 °C with stirring speed of 200 rpm. After the leaching process, the solution is filtrated, and the grey solution obtained was left overnight to get a clear solution. The solution was then added dropwise in 10% ammonia solution until the pH reaches 9. The precipitate is then collected and washed with deionized water and dried in an oven at 60 °C overnight. The dried deposit, i.e. EGA, was then calcined at 600 °C for 2 h. Before being used as catalyst support, EGA was characterized using surface morphology, XRD, and BET surface area analyses.

### 2.2. Preparation of Ni/EGA

10%Ni/EGA was synthesized via wet impregnation method. First, $Ni(NO_3)_2{\cdot}6H_2O$ was added into the beaker containing distilled water and left to dissolve. Then, EGA support was impregnated with the $Ni(NO_3)_2{\cdot}6H_2O$ solution. The solution was magnetically stirred for 3 h at 27 °C. The resulted product was subsequently dried at 110 °C for overnight. It was followed by a calcination process for 5 h at 600 °C with 5 °C $min^{-1}$ heating rate. Finally, the catalyst was allowed to cool in the fume hood before grounded and sieved at the desired particle size of 150 μm. The catalyst was then characterized by surface morphology, XRD, and BET surface area analysis.

### 2.3. GDR reaction

GDR reaction was conducted in a fixed-bed reactor at ambient pressure. The reactor tubing with internal diameter, ID = 0.95 cm and length, L = 30 cm was vertically positioned in a furnace. 0.2 g of catalyst was placed on the quartz wool in the middle of the reactor tube. Before the reaction starts, the catalyst was reduced for 1 h at 700 °C with the $H_2$ gas flowrate of 9.9 ml $min^{-1}$. Then, the reactant gas (i.e. $CO_2$) and glycerol were fed into the reactor. The liquid glycerol at a flowrate of 0.05 ml $min^{-1}$ was pumped into the upper end of the reactor tube by using an HPLC pump. The reaction temperature was set at 800 °C throughout the catalytic reaction under atmospheric pressure for 8 h. The outlet gas passes through the drierite bed before collected to remove the moisture content. The product was analyzed using Agilent 6890 gas chromatography (GC) equipped with a thermal conductivity detector. The following equation calculated the glycerol conversion and yield of hydrogen:

Glycerol conversion:

$$X_G = \frac{2F_{H_2} \times 4F_{CH_4}}{8F_{C_3H_8O_3}} \times 100 \quad [6]$$

Hydrogen yield:

$$Y_{H_2} = \frac{2F_{H_2}}{8F_{C_3H_8O_3}} \times 100 \quad [7]$$

## 3. Results and discussion

### 3.1. Characterizations of extracted γ-$Al_2O_3$

Four analyses were performed to analyze the presence of γ-$Al_2O_3$ after acid leaching process, which are the XRF, XRD, surface morphology and BET surface area.

a) X-Ray fluorescence (XRF) and X-Ray diffraction (XRD) analysis

Table 1 showed the compositions of aluminum dross and EGA. $Al_2O_3$ presents as the main component in the dross with a signification portion of 64.7%, followed by $CO_2$ (10.8%) and $N_2$ (9.58%). Meanwhile, the main composition of EGA is $Al_2O_3$ with 97% concentration, which confirmed the presence of $Al_2O_3$ as the main product extracted. The elements present in the aluminum dross and EGA was also evaluated and verified by XRD analysis to determine the type of $Al_2O_3$ produced. Fig. 1 represents the XRD pattern of aluminum dross and EGA. Fig. 1 (a) indicates the presence of various elements in the aluminum dross such as $Fe_2O_3$ (JCPDS card No: 00-039-1346), $Al_2O_3$ (JCPDS card No: 00-042-1468, Al (JCPDS card No: 00-004-0787), spinel $MgAlO_4$ (JCPDS card No: 00-005-0672), MgO (JCPDS card No: 00-004-0829), $SiO_2$ (JCPDS card No: 00-046-1045, aluminum nitride (AlN) (JCPDS card No: 00-025-1133)

**Table 1**
Compositions of aluminum dross and EGA.

| Chemical compositions | Aluminum Dross (wt.%) | Concentration of EGA (wt.%) |
|---|---|---|
| $Al_2O_3$ | 64.7 | 97 |
| $CO_2$ | 10.8 | – |
| $N_2$ | 9.58 | 1 |
| $SiO_2$ | 3.36 | – |
| $B_2O_3$ | 3.22 | – |
| $Fe_2O_3$ | 2.06 | 2 |
| MgO | 1.92 | – |
| $Na_2O$ | 1.07 | – |
| Cl | 0.387 | – |
| CuO | 0.271 | – |
| $TiO_2$ | 0.236 | – |
| $SO_3$ | 0.151 | – |
| Others | 2.245 | – |

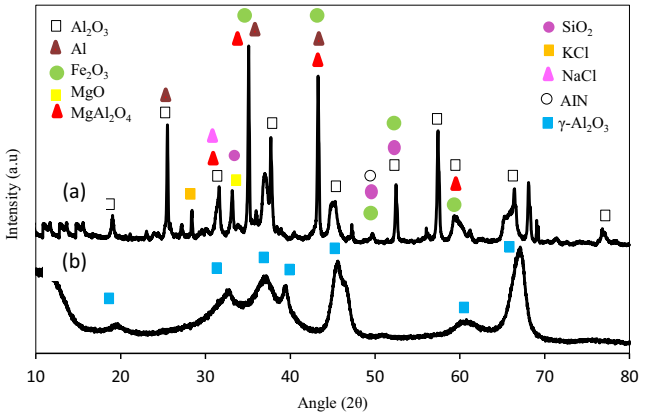


**Fig. 1.** X-ray diffractogram of (a) Aluminum dross (b) EGA.

and soluble salts such as KCl (JCPDS card No: 00-004-0587) and NaCl (JCPDS card No: 00-005-0628). Meanwhile, from Fig. 1 (b), the presence of $\gamma$-$Al_2O_3$ was detected at $2\theta = 19.8°$, 32.9°, 36.4°, 39.1°, 45.9°, 60.8° and 67.3° (JCPDS card No: 00-029-0063). This result is in agreement with How et al. [13] and Bahari et al. [14]. Besides, Fig. 1 shows that the crystallinity of $Al_2O_3$ (i.e. EGA) was lower compared to the aluminum dross. It might be due to the presence of different phase of $Al_2O_3$ in the aluminum dross. The presence of various phase of $Al_2O_3$ such as $\alpha$-, $\beta$- and $\gamma$- in aluminum dross lead to higher crystallinity of $Al_2O_3$.

**Table 2**
Physical properties of aluminum dross and EGA.

| Particles | Surface area ($m^2\ g^{-1}$) | Pore volume ($cm^3\ g^{-1}$) | Pore diameter (nm) |
|---|---|---|---|
| Aluminum Dross | 8 | 0.23 | 61.47 |
| EGA | 156.5 | 21.2 | 13.2 |

b) BET surface area and surface morphology analysis

BET surface area of the aluminum dross and EGA was tabulated in Table 2. As seen in Table 2, EGA showed higher specific surface area compared to aluminum dross. This condition is mainly due to the major presence of $Al_2O_3$ in the EGA with an insignificant number of impurities. The pore diameter of the aluminium dross is higher than EGA, which allow the company of other materials such as Si, Fe and Mg to attach inside the pore easily. Besides, the pore volume of the aluminium dross is lower compared to the EGA. It might be due to the existence of other metals on the pore of the aluminium dross and thus lead to the pore blockage and reduction in BET surface area. This result was confirmed by XRF and XRD analyses, as depicted in Table 1 and Fig. 1, where only 2% of $Fe_2O_3$ and 1% $N_2$ presented in EGA. In addition, the surface morphology shown by FESEM analysis represents a smoother surface of EGA compared to aluminum dross, as shown in Fig. 2 (b). Fig. 2 (a) demonstrated the existence of other elements on the surface of $Al_2O_3$, which contributed to the pore blockage and thus reduced the surface area. The EGA with a specific surface area of 156.5 $m^2\ g^{-1}$ was then used as catalyst support to synthesize 10%Ni/EGA.

### 3.2. Characterizations of catalyst

The synthesized catalyst was characterized by XRD, BET surface area and surface morphology analyses.

a) X-Ray diffraction (XRD) analysis

Fig. 3 shows the X-ray diffractogram of EGA and 10%Ni/EGA. The $\gamma$-$Al_2O_3$ appeared at the same $2\theta$ value even after the introduction of Ni into the support (refer section 3.1 (a)). For 10%Ni/EGA, the existence of two other components which are NiO and spinel $NiAl_2O_4$ was detected in the diffractogram. NiO possessed at $2\theta = 37.4°$, 43.5° and 63.3° (JCPDS card No: JCPDS card No: JCPDS 01-073-1519). Meanwhile, $NiAl_2O_4$ presence at 37.4° and 75.5° (JCPDS card No: JCPDS 00–010-0339). The presence of spinel phases, i.e. $NiAl_2O_4$ on the surface of catalyst indicated the strong interaction between metal and support due to the introduction of high temperature during the calcination process [15].

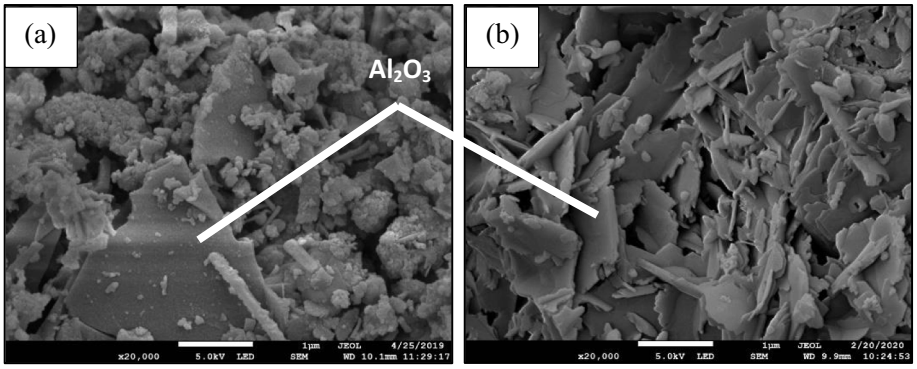


**Fig. 2.** FESEM image of (a) aluminum dross; (b) EGA.

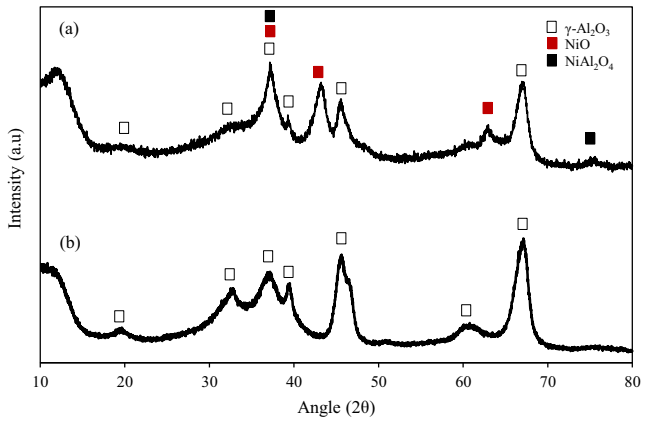


**Fig. 3.** X-ray diffractogram of (a) 10% Ni/EGA and (b) EGA.

b) BET surface area and crystallite size

The physical properties of EGA and 10%Ni/EGA was presented in Table 3. The addition of NiO into the support surface leads to a reduction in BET surface area from 156.5 to 108.3 $m^2$ $g^{-1}$. This result indicates the diffusion of metals on the support surface. The distribution of Ni into the porous surface of EGA support has led to the partial pore blockage and thus, reduced the BET surface area. Besides that, the increment in the pore diameter of 10%Ni/EGA (Table 3) was possibly due to the $Ni(NO_3)_2$ decomposition during the calcination process. At this stage, various porous structures have been formed where, the formation of higher pore diameter of 10%Ni/EGA has occurred. Nevertheless, the pore volume of 10%Ni/EGA was lower than EGA due to the accumulation of NiO particles within the pore structure.

The crystallite size of the 10%Ni/EGA is higher compared to EGA support, as depicted in Table 3. This result indicated the agglomeration of NiO particles on the surface of the catalyst. Commonly, small crystallite size indicates better metal dispersion into the support surface. But too small crystallite size tends to block the pores. Thus, 9.3 nm crystallite size of 10%Ni/EGA was sufficient to produce a catalyst with the best metal-support interaction.

c) Surface morphology

The morphology of the EGA at 20,000 magnification and 10%Ni/EGA catalyst at10000 magnifications are represented in Fig. 4. 10% Ni/EGA showed a bulky and rougher surface compared to EGA. Fig. 4(b) shows the encapsulation of small particles which indicates the accumulation of NiO on the surface of EGA. The XRD analysis verified the existence of NiO on the support surface.

### 3.3. Catalytic activity

A blank run was conducted over EGA. There is no significant increase in the glycerol conversion throughout the experimental work as depicted in Fig. 5. This result suggested that no gas-phase reaction occurred using EGA as a catalyst. The GDR was conducted at 800 °C under ambient pressure for 8 h with the 1:1 $CO_2$ to glycerol feed ratio. Fig. 5 shows the glycerol conversion using EGA and 10%Ni/EGA as catalysts. The glycerol conversion increased up to 22% when Ni metal introduced into the EGA support. As depicted in Fig. 6, hydrogen yield and CO yield obtained in this

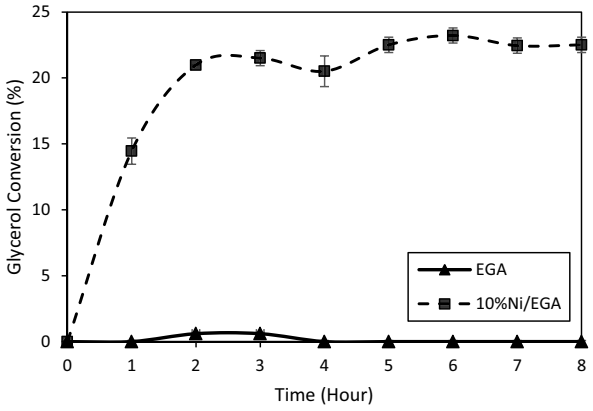


**Fig. 5.** Glycerol conversion of EGA and 10%Ni/EGA in GDR reaction.

**Table 3**
Textural properties of EGA support and 10% Ni/EGA.

| Particles | Surface area ($m^2$ $g^{-1}$) | Pore volume ($cm^3$ $g^{-1}$) | Pore diameter (nm) | Crystallite size (nm) |
|---|---|---|---|---|
| EGA | 156.5 | 21.2 | 13.2 | 5.37 |
| 10%Ni/EGA | 108.3 | 0.28 | 62.74 | 9.3 |

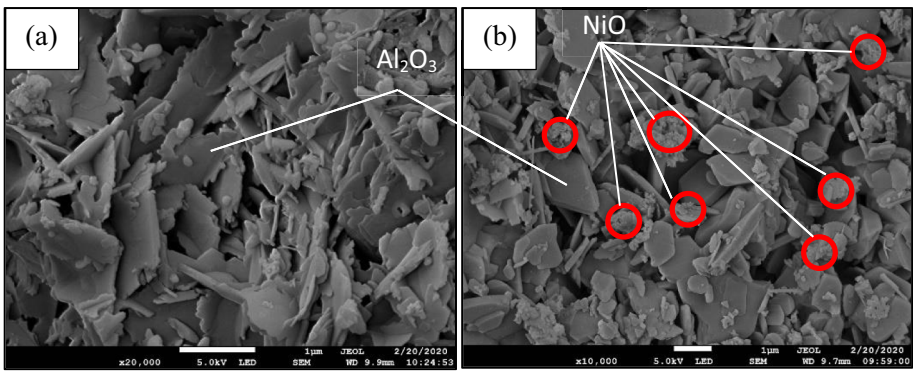


**Fig. 4.** FESEM image of (a) EGA and (b) 10%Ni/EGA.

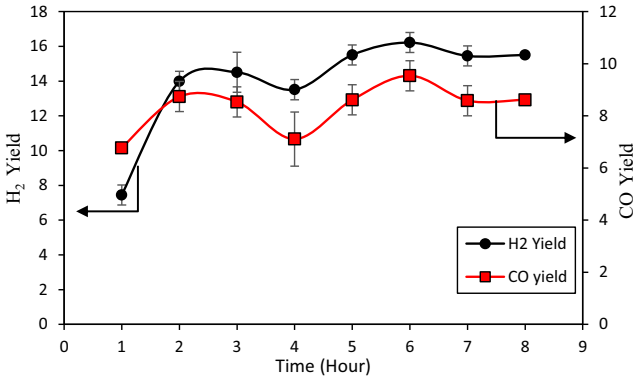


**Fig. 6.** $H_2$ and CO yield of 10%Ni/EGA in GDR reaction for 8 h reaction time.

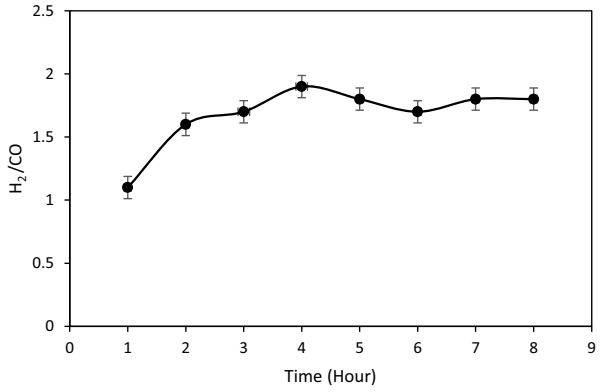


**Fig. 7.** $H_2$/CO ratio of 10%Ni/EGA in GDR reaction for 8 h reaction time.

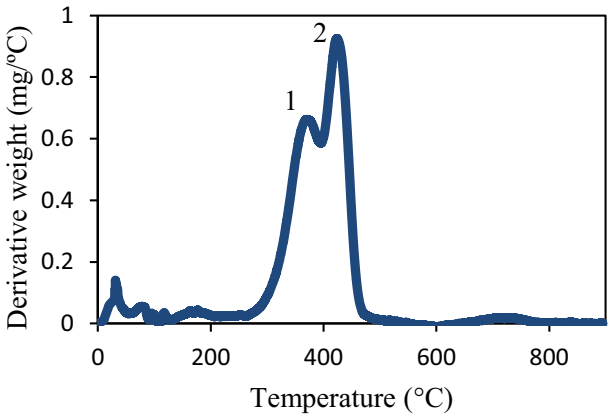


**Fig. 8.** TPO profiles of the spent catalyst of 10%Ni/EGA.

study were 15% and 8%. The increment in glycerol conversion, hydrogen yield CO yield is due to the good dispersion of Ni metal on the catalyst, small crystallite size and high specific surface area which enhanced the catalytic performance. Also, Ni metal and EGA support interactions help to increase catalyst stability. The conversion of glycerol, hydrogen yield and CO yield starts to be stable at 6–8 h. Fig. 7 displays the $H_2$/CO ratio for 8 h reaction time. The value obtained was varied from 1.1 to 1.8. The syngas produced at this ratio was suitable to be used as a feedstock for the Fischer-Tropsch synthesis in producing green fuels.

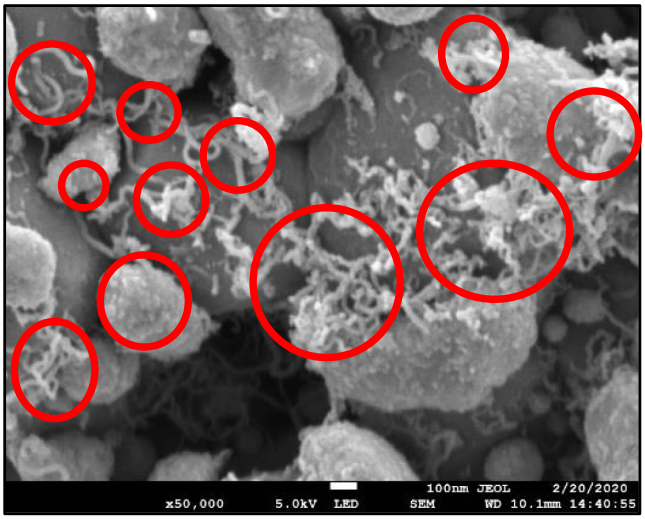


**Fig. 9.** FESEM microphotograph of the spent 10%Ni/EGA catalyst.

**Table 4**
EDX analysis of spent catalyst.

| Element | Weight (%) | Atomic (%) |
|---|---|---|
| Carbon (C) | 13.49 | 24.60 |
| Oxygen ($O_2$) | 29.18 | 39.95 |
| Aluminum (Al) | 32.03 | 26.00 |
| Nickel (Ni) | 25.30 | 9.44 |

### *3.4. Characterizations of spent catalyst*

The temperature-programmed oxidation (TPO) was carried out for the spent catalyst of 10%Ni/EGA to determine the amount of carbon present on the catalyst surface. Two peaks are presented between 300 and 500 °C in the TPO analysis, as shown in Fig. 8. According to the Chen et al. [16] and Gonzàlez et al. [17], the first peak (1) represents the oxidation of less ordered or more reactive carbon such as amorphous carbon. Meanwhile, the higher peak (2) described the gasification of more structural ordered or less reactive carbon such as graphitic carbon. The total weight loss obtained was approximately 0.78 mg which equivalent to 13.69%. This result indicates the decompositions of carbon.

Fig. 9 shows the morphology of spent 10%Ni/EGA. Filamentous-type and encapsulated solid carbons were clearly seen from the figure (i.e. in round red circle). Ni particles were found to cover by the multi-layer of carbon, and hence block the active site of the catalyst. This condition will lead to the reduction of catalytic activity within the time-on stream. Table 4 showed the EDX analysis of the spent catalyst. The weight of carbon was 13.49% which corresponds to the TPO analysis.

## 4. Conclusion

It can be concluded that γ-$Al_2O_3$ was successfully extracted from aluminum dross by acid leaching technique and utilized as catalyst support in the GDR reaction. EGA with the specific surface area of 156.5 $m^2$ $g^{-1}$ was used as catalyst support to synthesize 10%Ni/EGA by wet impregnation method. In the GDR reaction, 22% glycerol conversion and 15% hydrogen yield were achieved and therefore proved the excellent performance of EGA as catalyst support. The XRD, FESEM and BET surface area analyses showed good dispersion of metal in the catalyst matrices, which enhanced the performance of catalyst in the GDR. It is attributed to the small crystallite size of the EGA, high specific surface area and well dis-

persion of Ni on the catalyst support. From the analysis of spent catalyst, encapsulation of solid carbon and filamentous type of carbon was found on the catalyst surface. The presence of these carbon limiting the catalytic activity to achieve higher conversion of glycerol and syngas yield.

## CRediT authorship contribution statement

**Nurul Asmawati Roslan:** Formal analysis, Data curation, Investigation, Resources, Methodology, Writing - original draft, Writing - review & editing, Visualization. **Sumaiya Zainal Abidin:** Conceptualization, Supervision, Project administration, Funding acquisition, Writing - review & editing. **Nur Shafiqah Nasir:** Data curation, Writing - review & editing. **Chin Sim Yee:** Formal analysis, Resources. **Y.H. Taufiq-Yap:** Formal analysis.

## Declaration of Competing Interest

The authors declare that they have no known competing financial interests or personal relationships that could have appeared to influence the work reported in this paper.

## Acknowledgements

The authors would like to acknowledge Ministry of Higher Education, Malaysia for awarding the FRGS research grant vote FRGS/1/2018/TK02/UMP/02/12 and Universiti Malaysia Pahang (RDU1803118 and PGRS1903121) FRGS/1/2018/TK02/UMP/02/12 (RDU190197) for financial support.

## References

[1] P.S. Bulutoglu, Z. Say, S. Bac, E. Ozensoy, A.K. Avci, Appl. Catal. A 564 (2018) 157–171.
[2] C. Dang, S. Wu, G. Yang, Y. Cao, H. Wang, F. Peng, H. Yu, J. Energy Chem. 43 (2020) 90–97.
[3] S. Wang, Q. Wang, X. Song, J. Chen, Int. J. Hydrogen Energy 42 (2017) 838–847.
[4] M. Tavanarad, F. Meshkani, M. Rezaei, J. $CO_2$ Utilization 24 (2018) 298–305.
[5] K.W. Siew, H.C. Lee, J. Gimbun, S.Y. Chin, M.R. Khan, Y.H. Taufiq-Yap, C.K. Cheng, Renewable Energy 74 (2015) 441–447.
[6] H.C. Lee, K.W. Siew, M.R. Khan, S.Y. Chin, J. Gimbun, J. Energy Chem. 23 (2014) 645–656.
[7] Q. Ma, J. Sun, X. Gao, J. Zhang, T. Zhao, Y. Yoneyama, N. Tsubaki, Catal. Sci. Technol. 6 (2016) 6542–6550.
[8] A.K. Tripathy, S. Mahalik, C.K. Sarangi, B.C. Tripathy, K. Sanjay, I.N. Bhattacharya, Miner. Eng. 137 (2019) 181–186.
[9] A. Meshram, K.K. Singh, Resour. Convers. Recycl. 130 (2018) 95–108.
[10] M. Mahinrossta, A. Allahverdi, J. Environ. Manage. 223 (2018) 452–468.
[11] P. Ramaswamy, P. Tilleti, S. Bhattacharjee, R. Pinto, S.A. Gomes, Mater. Today Proc. 22 (2020) 1263–1273.
[12] L.F. How, A. Islam, M.S. Jaafar, Y.H. Taufiq-Yap, Waste Biomass Valorization 8 (2017) 321–327.
[13] Z. Zhang, T. Wei, G. Chen, C. Li, D. Dong, W. Wu, Q. Liu, X. Hu, Fuel 250 (2019) 176–193.
[14] M.B. Bahari, N.H.H. Phuc, F. Alenazey, K.B. Vu, N. Ainirazali, N.V. Dai-Viet, Catal. Today 291 (2017) 67–75.
[15] K.M. Hardiman, C.G. Cooper, A.A. Adesina, R. Lange, Chem. Eng. Sci. 61 (2006) 2565–2573.
[16] K. Chen, Z. Xue, H. Liu, A. Guo, Z. Wang, Fuel 113 (2013) 274–279.
[17] D. González, O. Altin, S. Eser, A.B. Garcia, Mater. Chem. Phys. 101 (2007) 137–141.